Wide-field fluorescence sectioning with hybrid speckle and uniform-illumination microscopy

Daryl Lim, Kengyeh K. Chu, and Jerome Mertz*

Department of Biomedical Engineering, Boston University, 44 Cummington Street, Boston, Massachusetts 02215, USA
**Corresponding author: jmertz@bu.edu*

Received May 22, 2008; accepted June 13, 2008;
posted July 14, 2008 (Doc. ID 96541); published August 6, 2008

We describe a method of obtaining optical sectioning with a standard wide-field fluorescence microscope. The method involves acquiring two images, one with nonuniform illumination (in our case, speckle) and another with uniform illumination (in our case, randomized speckle). An evaluation of the local contrast in the speckle-illumination image provides an optically sectioned image with low resolution. This is complemented with high-resolution information obtained from the uniform-illumination image. A fusion of both images leads to a full resolution image that is optically sectioned across all spatial frequencies. This hybrid illumination method is fast, robust, and generalizable to a variety of illumination and imaging configurations.

OCIS codes: 180.1790, 180.2520, 180.6900.

It is well known that standard wide-field fluorescence microscopy does not provide optical sectioning for laterally uniform objects (i.e., dc spatial frequencies) [1]. Several strategies have been devised to circumvent this problem, such as scanning confocal or structured illumination microscopies (see [2] and references therein). More recently, a strategy was demonstrated based on dynamic speckle illumination (DSI) [3–5], in which a series of images is acquired of a fluorescent object illuminated with random speckle patterns. Optical sectioning is then obtained by simply calculating the contrast of the image fluctuations in time. However, DSI microscopy is slow, since it generally requires several tens of images to produce a final sectioned image of reasonable quality. A possible strategy to speed up DSI microscopy is to use only a single speckle-illumination image and to calculate image contrast over space rather than time (i.e., over local resolution areas). However, such a single-shot technique, while fast, exhibits poor resolution.

In this Letter, we demonstrate a solution to these problems based on a hybrid double-shot technique that combines a single speckle-illumination (i.e., nonuniform) image I_n with a standard uniform-illumination image I_u. In this technique, I_n provides low-resolution information that exhibits optical sectioning at low spatial frequencies below a user-specified cutoff frequency κ_c, while I_u provides high-resolution information that exhibits optical sectioning above the cutoff frequency κ_c (or crossover frequency). By properly selecting κ_c and fusing low- and high-resolution information, we recover a final full resolution wide-field image that exhibits optical sectioning across the entire imaging bandwidth, including dc.

The setup of our hybrid technique is illustrated in Fig. 1 and is identical to that used in DSI microscopy. The phase front of a laser beam is randomized on transmission through a diffuser plate, and a resultant speckle pattern is projected into a sample via a microscope objective. Two fluorescence images are then acquired: one with the diffuser plate fixed (I_n) and another with the diffuser plate in motion (I_u). In the latter case, the speckle pattern is randomized so rapidly compared with the camera exposure time that I_u is equivalent to an image acquired with uniform illumination. The principle of our hybrid technique is to process both I_n and I_u to obtain a final optically sectioned high-resolution image. As a guide to our discussion, we will refer to Fig. 2, which illustrates the steps along the way.

As a first step, we consider $I_n(\vec{\rho})$ (Fig. 2(a)), where $\vec{\rho}$ are the image coordinates. Our goal in processing $I_n(\vec{\rho})$ will be to derive a low-resolution image that is optically sectioned even for dc frequencies. To this end we evaluate the local spatial contrast of $I_n(\vec{\rho})$, defined to be

$$C_N(\vec{\rho}) = \frac{\langle \sigma_n(\vec{\rho}) \rangle_A}{\langle I_n(\vec{\rho}) \rangle_A}, \tag{1}$$

where $\langle \sigma_n(\vec{\rho}) \rangle_A$ and $\langle I_n(\vec{\rho}) \rangle_A$ correspond, respectively, to the standard deviation and mean of $I_n(\vec{\rho})$ as calculated over a mosaic of local resolution areas A (each area assumed to be large enough to encompass several imaged speckle grains). To gain an intuitive un-

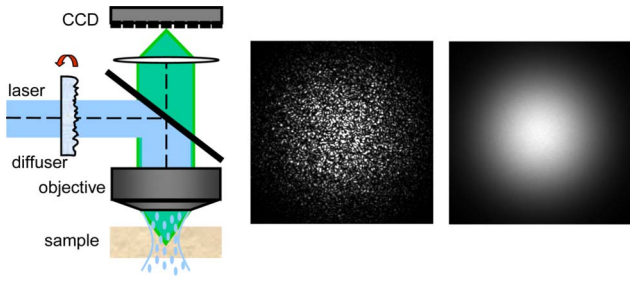

Fig. 1. (Color online) Microscope layout. A laser beam is sent through a diffuser plate, which is imaged onto the back aperture of the objective. The resultant sample fluorescence is imaged onto a CCD camera. Two images are acquired: with the diffuser plate stationary (speckle illumination, middle panel), and in rapid motion (uniform illumination, right panel).

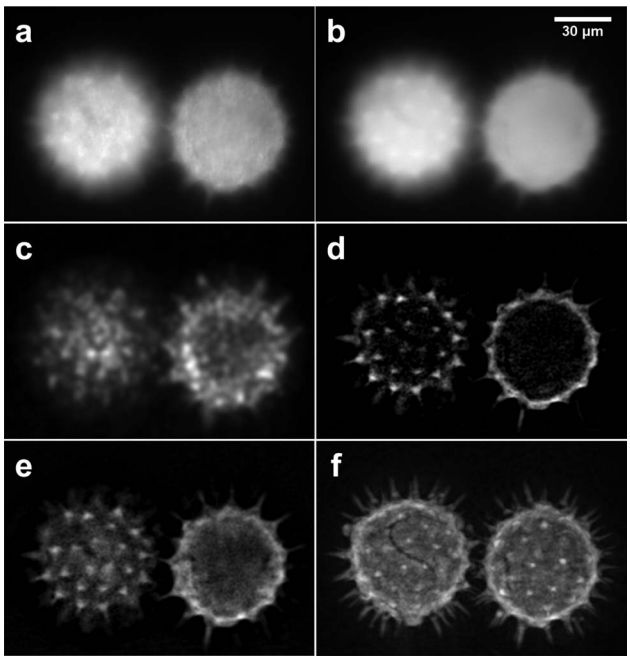

Fig. 2. Hybrid imaging technique applied to a pair of fluorescent pollen grains (Carolina Biological Supply) located at slightly different depths. a, Speckle-illumination image (I_n). b, Uniform illumination image (I_u). c, Intermediate low-pass image (I_{lp}). d, Intermediate high-pass image (I_{hp}) (note: negative values in this panel have been set to zero for ease of presentation). e, Composite full resolution optically sectioned image (I). f, Extended focus image obtained from a maximum intensity projection of 80 slices separated by 0.5 μm steps. The illumination source was a 488 nm argon laser (~3 mW at sample). All images in this paper were acquired with an Olympus 60×0.9 NA water-immersion objective and an exposure time of 200 ms per image. Panel c was obtained by using sliding resolution areas of size $A=7\times7$ pixels, corresponding to ~0.5 $\mu\mathrm{m}^2$ in the sample.

derstanding of $C_N(\vec{\rho})$, let us first consider a thin uniform object. In this case, $C_N(\vec{\rho})\approx1$ when the object is in focus (assuming that the illumination speckle pattern is fully developed [6], and the imaging resolution is high enough to easily resolve in-focus speckle grains); $C_N(\vec{\rho})\to0$ when the object goes out of focus. If we consider now a thick uniform object, then $C_N(\vec{\rho})$ thus corresponds to the relative proportion of $I_n(\vec{\rho})$ that can be interpreted as being in focus. Finally, making use of the uniform-illumination image $I_u(\vec{\rho})$, the product $C_N(\vec{\rho})I_u(\vec{\rho})$ can be interpreted as extracting only the in-focus contribution of $I_u(\vec{\rho})$ while rejecting out-of-focus contributions, at least on the coarse spatial scale defined by A.

However, an object is nonuniform in general, meaning that in fact two sources contribute to the measured contrast of $I_n(\vec{\rho})$, namely, speckle illumination and variations in the object itself. For our interpretation of contrast to be as object-independent as possible, we are interested only in the speckle-induced contrast. That is, we must correct Eq. (1) for any object-induced contrast contributions. To do this, let us examine the variations in I_n and I_u encompassed by an arbitrary resolution area A. Defining $O(\vec{\rho})$ to be the image intensity obtained from the actual object with a hypothetical uniform unit illumination, and $S(\vec{\rho})$ to be the image intensity obtained from a hypothetical uniform unit object with the actual speckle illumination, we may then make the following approximations:

$$I_n(\vec{\rho})\approx[\langle O\rangle_A+\delta O(\vec{\rho})][\langle S\rangle_A+\delta S(\vec{\rho})], \tag{2}$$

$$I_u(\vec{\rho})\approx[\langle O\rangle_A+\delta O(\vec{\rho})]\langle S\rangle_A. \tag{3}$$

In Eqs. (2) and (3) $\langle O\rangle_A$ and $\langle S\rangle_A$ arise from both in- and out-of-focus contributions of the object and illumination, whereas $\delta O(\vec{\rho})$ and $\delta S(\vec{\rho})$ must arise dominantly from in-focus contributions, since only these are well resolved [1] (the smaller the choice of A, the more tightly these latter contributions must be in focus). We then obtain the approximation

$$C_N^2\approx C_O^2+C_S^2+C_O^2C_S^2, \tag{4}$$

where C_O and C_S are, respectively, the contrasts associated with $O(\vec{\rho})$ and $S(\vec{\rho})$, as calculated over the resolution area A. Our goal, again, is to derive C_S. This is readily accomplished by using Eqs. (1) and (4), and also $C_O(\vec{\rho})=\langle\sigma_u(\vec{\rho})\rangle_A/\langle I_u(\vec{\rho})\rangle_A$. By performing such a derivation over all resolution areas, we finally obtain $C_S(\vec{\rho})$, which is a coarse-grained, object-independent measure of the relative proportion of $I_u(\vec{\rho})$ that is in focus. That is, the product $I_{su}(\vec{\rho})=C_S(\vec{\rho})\langle I_u(\vec{\rho})\rangle_A$ provides a low-resolution version of $I_u(\vec{\rho})$ that is optically sectioned even for dc frequencies. To summarize this first step of our algorithm, we have taken our speckle-illumination image $I_n(\vec{\rho})$, and from this we have extracted a speckle-induced contrast that provides a coarse-grained, optically sectioned version of $I_u(\vec{\rho})$. It should be noted that the extraction of speckle-induced contrast can be further improved with the use of wavelet prefiltering, as described in detail in [5], which has the effect of enhancing the rejection of out-of-focus background. Such wavelet prefiltering was applied in practice.

We now turn to the second step of our algorithm, which involves recovering higher-resolution information directly from the uniform-illumination image $I_u(\vec{\rho})$. To describe this step, it is more convenient to consider the Fourier transform of $I_u(\vec{\rho})$, denoted $\mathcal{I}_u(\vec{\kappa})$, where $\vec{\kappa}$ is spatial frequency. We recall that $\mathcal{I}_u(\vec{\kappa})$ does not exhibit optical sectioning for $\kappa=0$ (i.e., dc), but does for $0<\kappa<\kappa_{\max}$, where $\kappa_{\max}$ is the imaging bandwidth defined by the microscope aperture [1]. Thus, we specifically extract high-resolution (and therefore optically sectioned) information from $I_u(\vec{\rho})$ by applying a high-pass-filter, $\mathrm{HP}(\vec{\kappa})$, to $\mathcal{I}_u(\vec{\kappa})$ with cutoff frequency $\vec{\kappa}_c$ defined such that $\mathrm{HP}(\vec{\kappa}_c)=1/2$. We denote this high-pass-filtered version of $\mathcal{I}_u(\vec{\kappa})$ as $\mathcal{I}_{\mathrm{hp}}(\vec{\kappa})=\mathrm{HP}(\vec{\kappa})\mathcal{I}_u(\vec{\kappa})$. In practice, we use a Gaussian $\mathrm{HP}(\vec{\kappa})$.

The final step is to perform a fusion of the high-resolution information from $I_{\mathrm{hp}}(\vec{\rho})$ [where $I_{\mathrm{hp}}(\vec{\rho})$ is the inverse Fourier transform of $\mathcal{I}_{\mathrm{hp}}(\vec{\kappa})$] with the low-resolution information from $I_{su}(\vec{\rho})$. We begin by conditioning $I_{su}(\vec{\rho})$ such that its frequency content is ex-

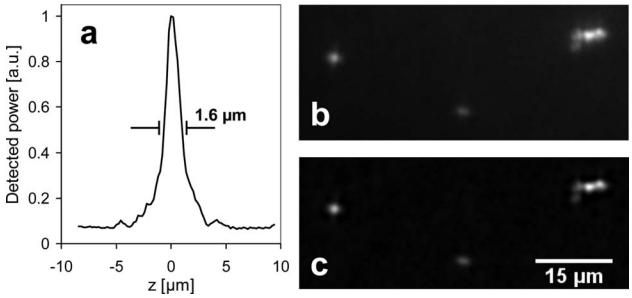

Fig. 3. a, Integrated signal from a thin fluorescent plane as a function of defocus z. b, Uniform-illumination image of 1 μm beads (Molecular Probes TetraSpeck Slide B). c, Processed hybrid image from speckle and uniform illumination.

actly complementary to that of $I_{\mathrm{hp}}(\vec{\rho})$. That is, we apply to $I_{su}(\vec{\rho})$ the low-pass filter, $\mathrm{LP}(\vec{\kappa})$, that is complementary to $\mathrm{HP}(\vec{\kappa})$ [i.e., $\mathrm{LP}(\vec{\kappa})=1-\mathrm{HP}(\vec{\kappa})$], obtaining $\mathcal{I}_{\mathrm{lp}}(\vec{\kappa})=\mathrm{LP}(\vec{\kappa})\mathcal{I}_{su}(\vec{\kappa})$, where $\mathcal{I}_{su}(\vec{\kappa})$ is the Fourier transform of $I_{su}(\vec{\rho})$. The intermediate images $I_{\mathrm{lp}}(\vec{\rho})$ and $I_{\mathrm{hp}}(\vec{\rho})$ are illustrated in Figs. 2(c) and 2(d).

To combine low-pass and high-pass information such that the transition across κ_c is seamless, we note that $\mathrm{LP}(\vec{\kappa}_c)=\mathrm{HP}(\vec{\kappa}_c)=1/2$ and introduce the scaling factor $\eta=|\mathcal{I}_{\mathrm{hp}}(\vec{\kappa}_c)|/|\mathcal{I}_{\mathrm{lp}}(\vec{\kappa}_c)|$, averaged over all angles of $\vec{\kappa}_c$. Finally, we define $\mathcal{I}(\vec{\kappa})=\eta\mathcal{I}_{\mathrm{lp}}(\vec{\kappa})+\mathcal{I}_{\mathrm{hp}}(\vec{\kappa})$, or, equivalently,

$$I(\vec{\rho})=\eta I_{\mathrm{lp}}(\vec{\rho})+I_{\mathrm{hp}}(\vec{\rho}). \tag{5}$$

$I(\vec{\rho})$ is our desired final image, illustrated in Fig. 2(e). This image combines both low- and high-frequency information (appropriately scaled) and also exhibits optical sectioning across the entire imaging bandwidth, including dc. The choice of η ensures that the optical transfer function, $\mathrm{OTF}(\vec{\kappa},z)$, associated with our hybrid imaging system varies smoothly across the cutoff frequency when $z=0$ (where z is defocus). To further ensure that there is no abrupt change in the OTF sectioning strength between low and high frequencies, the cutoff frequency was chosen such that the FWHM of $\mathrm{OTF}(\vec{0},z)$ and $\mathrm{OTF}(\vec{\kappa}_c,z)$ are about the same. In practice, this means that the cutoff frequency was chosen to be very roughly $|\vec{\kappa}_c|\approx 0.2\kappa_{\max}$. We note that since C_S depends linearly on fluorophore concentration [3], so does $I_{su}(\vec{\rho})$. Moreover, since all further operations on $I_{su}(\vec{\rho})$ and $I_u(\vec{\rho})$ in the construction of $I(\vec{\rho})$ are linear, $I(\vec{\rho})$ also depends linearly on fluorophore concentration.

We emphasize that only two shots, $I_n(\vec{\rho})$ and $I_u(\vec{\rho})$, were required for generating $I(\vec{\rho})$, which in principle can be acquired quite rapidly (in our case, 200 ms per shot). To demonstrate that our hybrid technique indeed provides optical sectioning at dc, we imaged a thin, uniform fluorescent plane. Figure 3(a) illustrates the integrated intensity in $I(\vec{\rho})$ as a function of the plane defocus z. The FWHM of the optical sectioning trace is 1.6 μm. The expected scaling law for the optical sectioning trace can be derived following a similar calculation as provided in [5], though this time evaluating speckle contrast in space rather than in time. Based on the Stokseth approximation for $\mathrm{OTF}(\vec{\kappa},z)$ [7], we obtain a sectioning strength given by $|z|^{-3/2}$, which is close to the $|z|^{-2}$ sectioning strength exhibited by an ideal confocal microscope. To further demonstrate that our hybrid technique indeed provides high-resolution imaging similar to conventional wide-field microscopy, we imaged 1 μm fluorescent beads on a glass slide. Figures 3(b) and 3(c) exhibit essentially identical resolution (the leftmost bead exhibits the same FWHM in both images), the latter outperforming the former owing to a rejection of background fluorescence haze.

In summary, we have described a two-shot hybrid imaging technique that combines the advantages of speckle and uniform illumination. Speckle illumination provides low-resolution image structure that exhibits optical sectioning even at dc. Uniform illumination provides a complementary high-resolution image structure that also exhibits optical sectioning with a commensurate scaling law as a function of defocus. The combination of both images thus provides optical sectioning across the full imaging bandwidth, since, in effect, the speckle-illumination image has served to fill in the missing cone present in the frequency support of the uniform-illumination image. The advantage of our hybrid technique over DSI microscopy is that it is significantly faster, requiring only two shots rather than several tens of shots, making it easily amenable to video rate imaging. The advantage over confocal microscopy is its simplicity, robustness, ease of implementation in any wide-field microscope setup, and versatility. For example, the illumination can be delivered directly to the sample independently of the imaging optics. As a final note, we point out that our technique of generating a low-resolution optically sectioned image is not restricted to the use of speckle illumination and can be generalized to any type of patterned illumination, random (such as speckle) or nonrandom (such as a periodic grid or checkerboard pattern). The crux of our technique is the accurate combination of this low-resolution image with a complementary high-resolution image obtained from uniform illumination.

This work was partially supported by the National Institutes of Health (NIH; R21 EB007338).

References

1. N. Streibl, Optik (Stuttgart) **66**, 341 (1984).
2. J. B. Pawley, *Handbook of Biological Confocal Microscopy* (Plenum, 2006).
3. C. Ventalon and J. Mertz, Opt. Lett. **30**, 3350 (2005).
4. C. Ventalon and J. Mertz, Opt. Express **14**, 7198 (2006).
5. C. Ventalon, R. Heintzmann, and J. Mertz, Opt. Lett. **32**, 1417 (2007).
6. J. W. Goodman, *Speckle Phenomena: Theory and Applications* (Roberts & Company, 2006).
7. P. A. Stokseth, J. Opt. Soc. Am. **59**, 1314 (1969).